

# Debris Evolution and Lifetime Following an Orbital Breakup

V. A. Chobotov\* and D. B. Spencer†

*The Aerospace Corporation, El Segundo, California 90245*

This paper is an overview of the space debris modeling techniques and tools used at The Aerospace Corporation in support of the Air Force space debris efforts. A discussion is presented of the software tools IMPACT, which does the breakup analysis, and DEBRIS, which does collision hazard assessment. Additionally, some effects of atmospheric drag on debris environment are presented.

## Nomenclature

$A$	= projected area of the spacecraft
$d$	= distance traveled through the cloud
$E'$	= loss in energy due to heat and light
$M_e$	= empirical function of the collision velocity
$M_i$	= mass of $i$ th object
$m_i$	= mass of $i$ th particle (fragment)
$N$	= number of fragments of mass $m$ and greater
$n_i$	= number of particles moving at a velocity
$Q$	= energy for the spread of fragments
$V$	= volume of cloud
$V_i$	= velocity of $i$ th object
$V_{rel}$	= relative velocity at collision
$v_i$	= velocity of $i$ th particle
$v_r$	= velocity of spacecraft in the cloud
$\rho$	= density of particles in the cloud

## Introduction

THE purpose of this paper is to describe the space debris modeling efforts (past and present) performed for the U.S. Air Force Space Systems Division by the Space Hazards Section of The Aerospace Corporation.

The need for modeling orbital breakups and the resultant debris evolution was recognized when planning was underway for the antisatellite (ASAT) test (the first against a live target). The Solwind satellite (P78-1), chosen as the target, was a solar observation satellite that was launched in 1978 into a sun-synchronous orbit. The intercept took place off the west coast of the United States on September 13, 1985. Several pieces of debris were tracked following the event, and several thousand more were predicted but were not tracked due to their small size. In this test, a large orbiting object collided with a small projectile on a ballistic trajectory.

In 1986, the Delta-180 mission called for a collision in orbit of a payload with the second stage that put it into orbit. This was the first test of its kind in which two objects of roughly similar size collided in space.

The determination of the collision hazard to other spacecraft by a debris-producing event was also necessary. This paper presents a description of the basic algorithms used in program IMPACT and the dynamics of an orbiting debris cloud as it is modeled in the program DEBRIS. The former

program determines the event's breakup characteristics, whereas the latter determines the probability of collision when a resident space object enters the debris cloud. These tools were developed to examine the short-term hazard to spacecraft following an orbital breakup.

Also, the study of debris evolution and lifetime is important in assessing the collision hazard posed to other spacecraft by a debris-producing event. An example is presented of the effect of the ballistic coefficient and the atmospheric characteristics on the lifetime of particles.

## Background and Past Experiences

The work in the area of space debris at The Aerospace Corporation dates back to 1979 and has increased dramatically since just before the 1985 ASAT test. The emphasis of the research has been in the area of modeling explosions and collisions, as well as studying the collateral hazard posed to other spacecraft as a consequence of orbital breakups.

On September 13, 1985, the Air Force made the first actual test of their air-launched ASAT weapon. The P78-1 satellite weighed approximately 850 kg and was in a sun-synchronous orbit at an altitude of approximately 500 km. The ASAT was placed on a ballistic trajectory that crossed the orbital path of the satellite; the two objects collided broadside with a relative velocity of approximately 7 km/s. This collision fragmented the satellite, as planned.

The Space Hazards Section of The Aerospace Corporation predicted the breakup characteristics of the satellite. The prediction was for 315 fragments > 10 cm in size remaining after one orbital revolution of the target's orbit. Also predicted were 685 fragments > 10 cm re-entering within 1 revolution. Observations showed that there were 257 fragments after 1 revolution in the target's orbit. No center-of-mass cloud was observed, which leads to the conclusion that there was a low-momentum transfer during the collision. The maximum fragment altitude reached was 2800 km.

On September 5, 1986, the Strategic Defense Initiative Organization (SDIO) conducted an experiment in space. A 930-kg payload was put into orbit atop a Delta booster. Once in orbit, the Delta second stage detached from the payload. The payload collided with the 1370-kg Delta second stage with a relative velocity of approximately 3 km/s. This took place at an altitude of approximately 200 km.

The Space Hazards Section again was called upon to perform a collision hazard assessment prior to this mission. The ratio of the masses of the two bodies was approximately 3:2. Both were orbital, and so the theory that was developed for the P78-1 test needed further development. Because of the size ratios, a direct head-on collision was not very likely. Instead, a side swipe or glancing-blow collision was predicted. The study predicted that 300 fragments > 10 cm would remain after 1 revolution of the target orbit, 700 fragments would re-enter within 1 revolution, and  $1 \times 10^6$  particles > 1 mm would be produced.

Presented as Paper 90-0085 at the AIAA 28th Aerospace Sciences Meeting, Reno, NV, Jan. 8-11, 1991; received Jan. 30, 1990; revision received Jan. 28, 1991; accepted for publication Feb. 2, 1991. Copyright © 1990 by the American Institute of Aeronautics and Astronautics, Inc. All rights reserved.

\*Manager, Space Hazards Section, P.O. Box 92957. Associate Fellow AIAA.

†Member of Technical Staff; currently, Graduate Student, Department of Aerospace Engineering Sciences, Campus Box 431, University of Colorado at Boulder, Boulder, CO 80309. Member AIAA.

Space surveillance network observations showed that 320 observable fragments remained in orbit after two days. No center-of-mass cloud was observed, which, like the P78-1 test, indicated a low-momentum transfer. The maximum fragment altitude reached was 2000 km.

### Spacecraft Breakup Modeling

Much of the theory behind breakup modeling was derived from a series of laboratory tests and the two orbital tests described previously.

In the cases of the head-on, the glancing-blow, and the explosion scenarios, the objective of modeling is to determine the number of fragments, their size, and their velocities. Once the number and velocity distributions are determined, the orbital elements of the fragments can be obtained. These, in turn, define the debris cloud and its evolution in time. The underlying theory of the modeling, as is implemented in the program IMPACT, is outlined in general as follows.

### Spread Velocity and Number of Fragments Distribution

#### Inelastic Energy of Collision

Consider a case in which two masses  $M_1$  and  $M_2$ , moving at velocities  $V_1$  and  $V_2$ , collide inelastically. From the conservation of momentum

$$M_1 V_1 + M_2 V_2 = (M_1 + M_2) V_{cm} \quad (1)$$

where  $V_{cm}$  is the velocity of the center of mass.

Conservation of kinetic energy yields the following equation

$$\frac{1}{2} M_1 V_1^2 + \frac{1}{2} M_2 V_2^2 = \frac{1}{2} (M_1 + M_2) V_{cm}^2 + Q \quad (2)$$

This can be related to fragment mass and spread velocity by the relation

$$Q = \frac{1}{2} \sum_i m_i v_i^2 + E' \quad (3)$$

The center of mass is moving with velocity  $v_{cm}$ ; at the same time, fragments are spreading with respect to the center of mass. For the case in which  $E' = 0$ ,  $Q$  depends on the relative velocity of impact and the ratio between the two colliding masses. It can be obtained from the relation

$$Q = F \cdot (KE)_{rel} \quad (4)$$

where  $(KE)_{rel} = (\frac{1}{2}) M_1 V_{rel}^2$ . The fraction  $F$  is related to mass ratio  $R$  ( $R = m_2/m_1$ ), as shown in Fig. 1. Once the value of  $Q$  is determined, the problem is to determine fragment mass and assign the spread velocities to satisfy Eq. (3).

### Breakup Scenarios

From study of the P78-1/ASAT and Delta-180 missions, three breakup models were developed. The head-on collision was developed for a small object colliding with a large object. The glancing blow was used for the collision of two similarly sized objects. The explosion model was used for either an explosion due to a pressure buildup in a tank or a detonation. The cumulative number of fragments produced is found using empirical relationships.

#### Head-On Collision

The analysis of a head-on collision begins with data taken from the initial conditions of the collision (state vectors and masses of colliding objects). The cumulative number of objects produced is given in Ref. 1 as an empirical relationship of the closing velocity and the mass of the smaller object in the collision

$$N = K \left( \frac{m}{M_e} \right)^{-0.75} \quad (5)$$

Here,  $M_e = k M_p V_{rel}^2$ , where  $k$  is a constant with unity value and units of (time/distance)<sup>2</sup> and  $K$  is the constant that depends on the rigidity of the material. For collisions between satellites, Ref. 1 has determined that  $K \approx 0.45$  is a good value to use since it appears that there is good correlation between experimental and theoretical results when this value of  $K$  is used.

#### Glancing-Blow Collision

The glancing-blow scenario is a combination of the explosion and the colliding scenarios. Assume that the two objects are colliding off their centerline (Fig. 2). When the collision occurs, parts of the two bodies come into direct contact with each other. Momentum overcomes the adhesion of the two bodies and shears off the parts in contact. The parts in the direct contact region then act like two objects involved in a head-on collision. The remaining parts also break up from the shock waves produced by the shearing. These shock waves are similar to those produced by an explosion and so the spread velocities are found using the methods developed for the head-on and explosion scenarios.

#### Explosion Model

Fragments generated by explosions have a different size distribution than fragments generated by collision. Again from Ref. 1, the number of fragments generated by an explosion is a piecewise continuous function of the fragment mass,

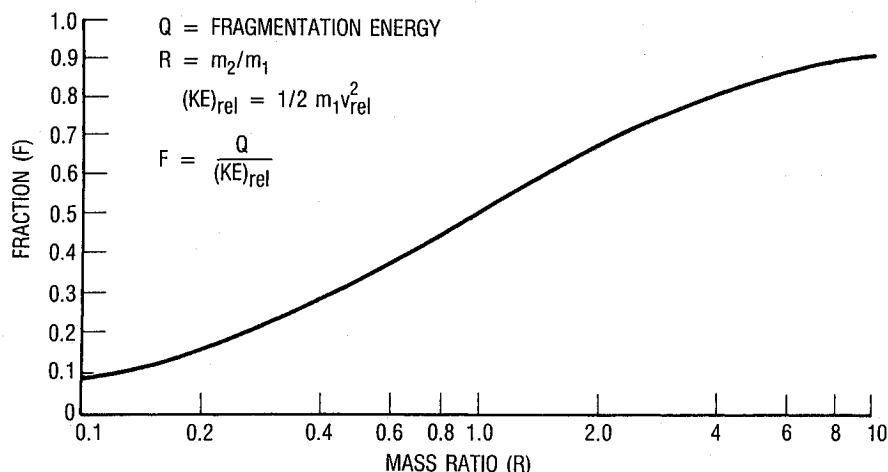


Fig. 1 Inelastic collision energy fraction  $F$  vs mass ratio  $R$ .

the satellite mass, and the energy available for breakup. Thus,

$$N = 1.71 \times 10^{-4} M_e \exp(-0.02056m^{1/2}) \quad \text{for } m > 1936 \text{ g}$$

$$= 8.69 \times 10^{-4} M_e \exp(-0.0576m^{1/2}) \quad \text{for } m \leq 1936 \text{ g} \quad (6)$$

#### Laboratory Results

Figure 3 is a typical example of fragment distribution vs size. It has been taken from Ref. 2 and is based on the result of a laboratory experiment. In this experiment, a 237-g projectile was used to impact a target of 25 kg mass at a relative velocity of 3.3 km/s. The cumulative number of fragments vs the diameter of the fragment is shown in this plot. Figure 3 illustrates two regions termed collision and explosion distributions resulting from the involved masses of the colliding objects and the breakup of the remaining structure.

Size of the fragments depends on the mass density. For satellite structures, the density could vary from 0.1 to 5 g/cm<sup>3</sup>. The fragment mass density distribution will vary, depending on the physical properties of colliding objects.

#### Velocity Distributions

An important item of information needed in determining the shape of an orbiting debris cloud following a breakup is the distribution of spread velocities of the debris particles emanating from the center of mass of the system. Previous work assumed that all particles of the same size moved at the same velocity, as shown in a representative graph in Fig. 4. In reality, for a given size, several fragments are moving faster while others are moving slower. A more realistic approach to the modeling of the velocity distribution must therefore take into account the velocity variation for a given size particle. This has been implemented in the program IMPACT as follows.

#### Determination of Fragment Spread Velocity

The spread velocities of the fragments must satisfy Eq. (3). To obtain a relationship between a smaller fragment mass with

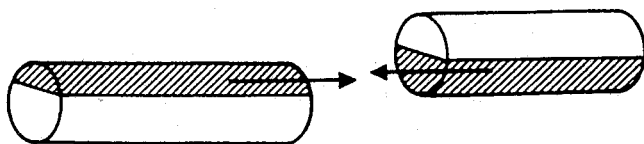


Fig. 2 Glancing-blow geometry.

its velocity and a larger mass fragment with its velocity, it may be assumed that the kinetic energies are equally imparted to each fragment such that

$$\frac{1}{2} m_1 v_1^2 = \frac{1}{2} m_2 v_2^2 \quad (7)$$

from which it follows that

$$\frac{v_2}{v_1} = \left( \frac{m_1}{m_2} \right)^{1/2} \quad (8)$$

This assumption breaks down for smaller-size fragments (<0.1 cm) because, as the area on which pressure is applied by the shock wave becomes very small, the effectiveness of the shock wave is reduced. For large-sized fragments, this assumption is in general agreement with some laboratory tests and other results shown in Fig. 5. Three curves are shown in this plot. One is for the nominal case, and the others are for extreme cases showing approximate upper and lower limits of the spread velocities of the fragments. The spread velocities of the smallest fragments, thus, are seen to be limited to 1.3 times the impact velocity, whereas the larger fragments may have velocities generally between the upper and lower limits of the curves in Fig. 5.

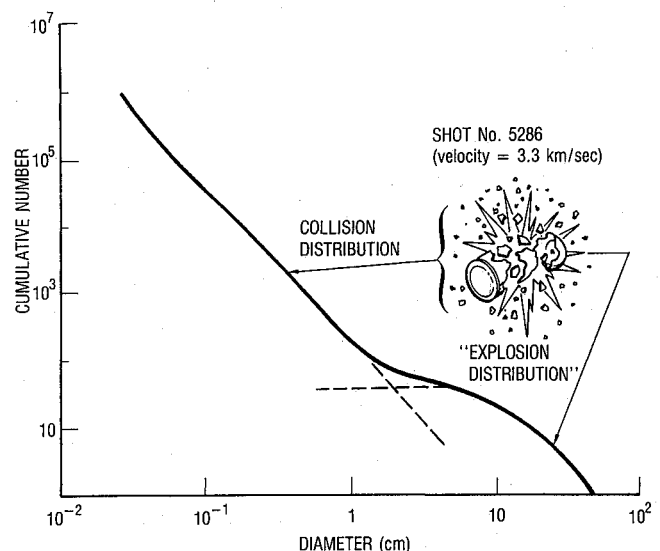


Fig. 3 Number of fragments produced from 237-g projectile.

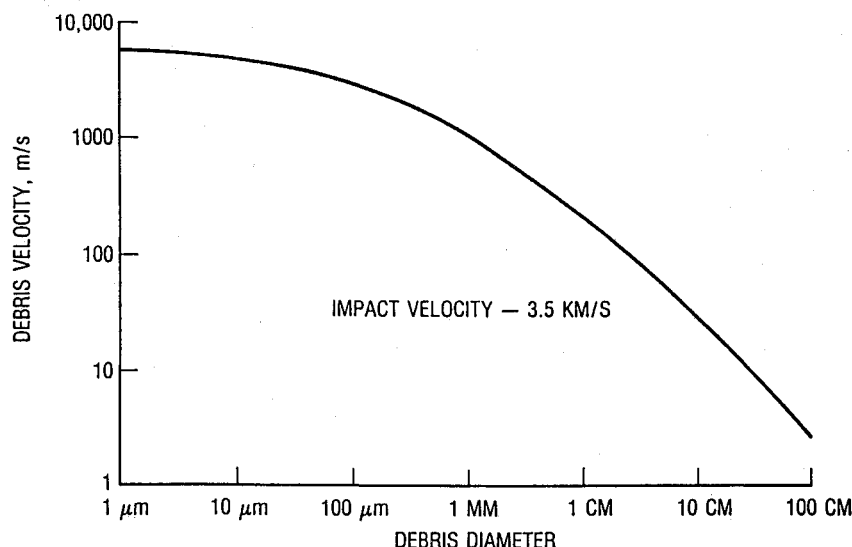


Fig. 4 Idealized model of velocity distribution.

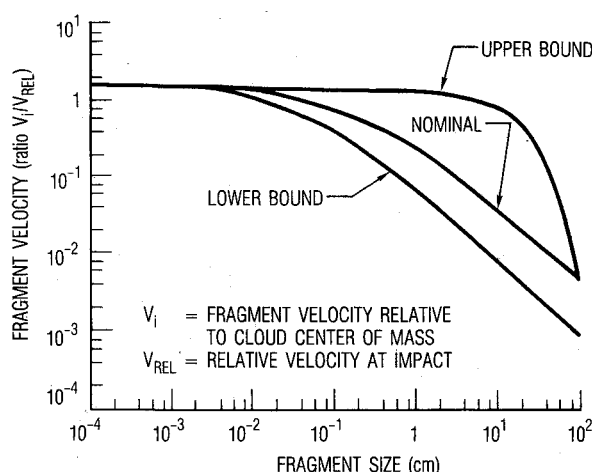


Fig. 5 Model: On-orbit debris total velocity for body-to-body impact.

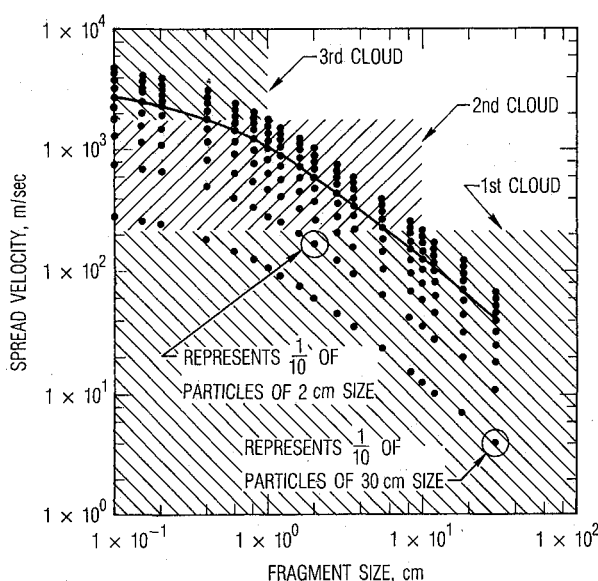


Fig. 6 Distributed velocity characteristics.

#### Distribution of Fragment Spread Velocities

The velocity variation of a given size (mass) fragment can be modeled in different ways. One approach is to assume that the difference in the velocity variation of a given size fragment is constant from the lowest to the highest velocity of the fragment. If, for example, there are  $n$  fragments of equal size with mass  $m$  for which the characteristic (average) spread velocity is  $V_i$  (as given in Fig. 5, for example), then the relative kinetic energy of the fragments is given by the equation

$$KE = \frac{1}{2}(nm)V_i^2 \quad (9)$$

By conserving energy and assuming that the particles move at  $k$  different velocities,

$$KE = \frac{1}{2}m \sum_{i=1}^k n_i V_i^2 \quad (10)$$

If different velocities are evenly spread out, then

$$v_i = v_1 + \Delta(i-1) \quad (11)$$

where  $\Delta$  is a linear velocity increment and  $v_1$  may be assumed as some fraction of  $V_i$  such as 10%.

#### Average Velocity

Following an orbital breakup, there are particles moving away at many different velocities. This also can be thought of as many different debris clouds superimposed over each other. For practicality, however, only three debris clouds superimposed on each other are selected. Choosing two break points, e.g., sizes of 1 and 10 cm, the total kinetic energy of all particles of sizes  $>10$  cm, between 1 and 10 cm, and below 1 cm can be calculated. Given the total energy and the total mass in these ranges, an average velocity can be found in the form

$$v_{ave}^2 = \frac{\frac{1}{2} \sum_{i=1}^N m_i n_i v_i^2}{\frac{1}{2} \sum_{i=1}^N m_i n_i} \quad (12)$$

where the denominator is the sum of all particle masses in the desired range, i.e., above 10 cm, 1–10 cm, or below 1 cm. This yields three values of average velocities, corresponding to each of the three debris clouds.

#### Number of Particles per Cloud

At each of the break points, there are  $k$  velocities associated with fragments of that size. These velocities are defined in Eq. (11). Two different velocities are determined, each representing the maximum velocity that a fragment of size 1 and 10 cm, respectively, could have.

When Eq. (9) is equated with Eq. (10) and Eq. (11) is inserted, the  $\Delta$  variable can be determined; thus, the velocities of each fragment can be found. If these particles are ranked in ascending order by velocity, the distribution of all of these pieces can be estimated. Using the maximum velocities at the break points, one can determine the cutoff points that would distinguish one cloud from another. When the maximum velocity for the 10-cm break point is taken, all fragments of all sizes whose spread velocity is  $< v_{max}$  are included in the slowest moving debris cloud. Similarly, all debris fragments falling between the maximum velocity for the 10-cm break point and the maximum velocity for the 1-cm break point are included in the middle evolving debris cloud. Finally, all fragments that are moving faster than the maximum velocity at the 1-cm break point are counted in the fastest evolving debris cloud.

#### Results

An example of the results is shown in Fig. 6. This figure is a plot of spread velocity vs fragment size. The solid line is for the spread velocity that is associated with the single velocity for a particular size (see Fig. 4). In this case,  $k = 10$ , so that

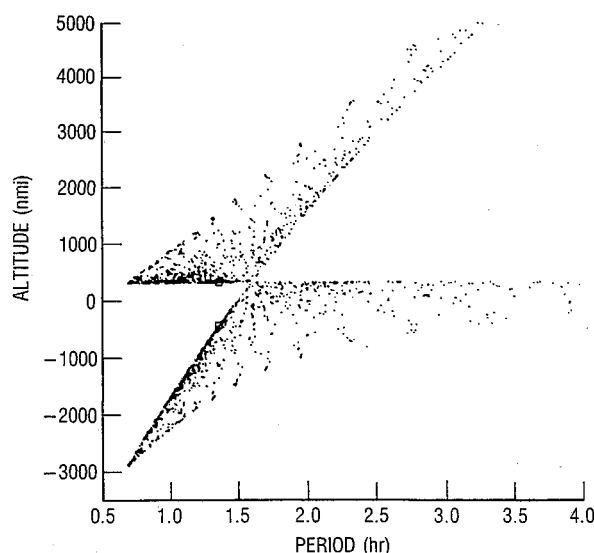


Fig. 7 Apogee and perigee altitudes of each fragment vs its period:  $MR = 15$ ;  $NF = 992$ .

each dot represents 10% of the number of particles of that size. For each vertical column of particle velocities, it can be thought of also as an equipartition of kinetic energy above and below the solid line.

#### Computing Fragment Directions and Orbits After Collision

There are three steps in the method of analysis to determine the fragment orbits: 1) determine the orbit of the center of mass of the two objects colliding; 2) calculate the masses, velocities, and directions of the fragments relative to the center of mass; and 3) input the results into an orbit element conversion program to compute orbital parameters of the fragments that would allow analysis and generation of plots and tables. Program IMPACT was written to perform these steps using the breakup model previously described. The results from program IMPACT are available in tabular or plot form.

An example of a plot is the Gabbard diagram illustrated in Fig. 7.<sup>3</sup> A Gabbard diagram is a plot of fragment apogee and perigee altitudes vs orbital period and is plotted for a large number of fragments following an orbital breakup. The diagram can be thought of as resembling a butterfly (for a circular orbital breakup), with the center body located at the altitude and period of the object breaking up, and the upper and lower wings representing the apogee and perigee altitudes, respectively. For an object breaking up in an elliptical orbit, the two wings no longer are connected.

#### Debris Cloud Modeling in Circular Orbits

The modeling of a debris cloud resulting from an orbital breakup in a circular orbit has been described in Refs. 3-5. Linearized equations for relative motion in orbit were used to obtain the trajectories of the fragments with given initial velocity distributions. The volume of the cloud was expressed in closed form as a function of time up to the time of the closure of the cloud around the Earth. The density of the fragments in the cloud was obtained for the number of fragments calculated in program IMPACT.

Figure 8 illustrates the toroidal form of the fragment orbits about the Earth. The pinch point in Fig. 8 denotes the position of the original breakup. Since all fragments must pass through this point at different times and since the fragment orbits are affected by perturbations, the pinch point and the torus begin to spread until eventually the orbits envelop the Earth.

The analytical representation of the cloud and its evolution in time, including drag effects, is described briefly in this section as is implemented in program DEBRIS.

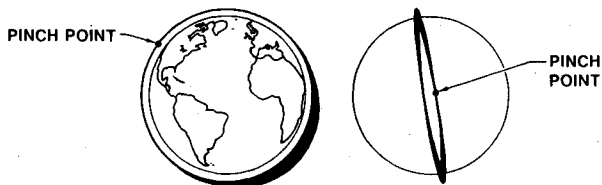


Fig. 8 Cloud trajectories in torus form.

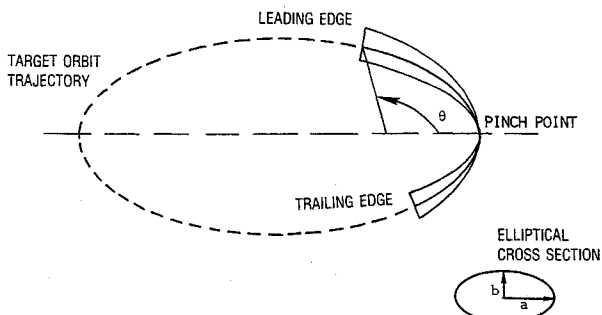


Fig. 9 Pinched torus model.

#### Cloud Volume Description

Previously published studies<sup>3,4</sup> show that the volume of a debris cloud in a circular orbit can be expressed approximately in the form

$$V_1(t, \theta) = \frac{4\pi}{3} |\det[M]| \left( \frac{\Delta v}{\dot{\theta}} \right)^3 \quad (13)$$

where

$$M = \begin{bmatrix} a_{11} & a_{12} & 0 \\ -a_{12} & a_{22} & 0 \\ 0 & 0 & a_{33} \end{bmatrix}$$

$$a_{11} = -3\theta + 4 \sin \theta$$

$$a_{12} = 2(1 - \cos \theta)$$

$$a_{22} = \sin \theta$$

$$a_{33} = \sin \theta$$

where  $\theta$  and  $\dot{\theta}$  are the angle and its rate swept out by the rotating reference frame with respect to the inertial frame, as shown in Fig. 9. The matrix  $[M]$  is the state transition matrix relating relative position to initial spread velocity  $\Delta v$ .

The volume of the debris cloud also may be represented as a function of time in the form

$$V_2(t, \theta) = \pi a(t, \theta) b(t, \theta) L(t) \quad (14)$$

where

$$a(t, \theta) = \sqrt{a_{12}^2 + a_{22}^2} \left( \frac{\Delta v}{\dot{\theta}} \right)$$

= semimajor axis of torus cross section

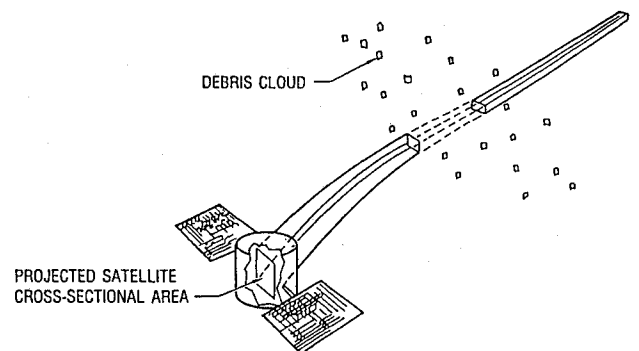
$$b(t, \theta) = a_{33} \left( \frac{\Delta v}{\dot{\theta}} \right)$$

= semiminor axis of torus cross section

$$L(t) = (\dot{L}_1 + \dot{L}_2)t$$

= in-plane arc distance between the leading and trailing edge of the debris cloud

Here  $\dot{L}_1$  and  $\dot{L}_2$  are leading- and trailing-edge growth rates, respectively, for all times  $t \leq t_{cl}$  where  $t_{cl}$  is the time at which



- $PROB_{COLLISION} = SATELLITE\ AREA \times DEBRIS\ DENSITY \times DISTANCE\ THRU\ CLOUD$
- DISTANCE THRU DEBRIS CLOUD IS A FUNCTION OF MUTUAL INCLINATION BETWEEN SATELLITE AND DEBRIS ORBITS
- DEBRIS DENSITY DECREASES AS CLOUD EXPANDS
- PROBABILITY OF COLLISION INVERSE FUNCTION OF TIME AFTER INTERCEPT

Fig. 10 Spacecraft passing through cloud.

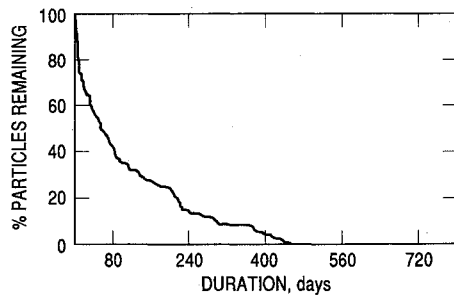


Fig. 11 Orbital lifetimes of debris particles.

$$F_{10.7} = 75, \Delta V = 100 \text{ m/sec}$$

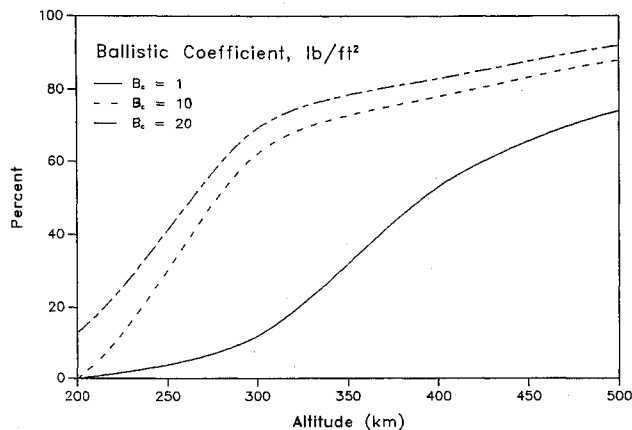


Fig. 12 Percent of particles remaining after one month.

the torus closes. The maximum values of  $a(t, \theta)$  and  $b(t, \theta)$  are defined when  $\theta = \pi/2$  (one-quarter revolution after breakup). The decrease at the pinch point ( $\theta = 0$ ) and at  $\theta = \pi$  thus defines the envelope (torus) of the fragment orbits.

The smaller of the two volumes  $V_1$  is used for computation of the density in the cloud. However, if  $t > t_{cl}$ , the  $V_2$  is always used as the volume of the debris cloud. The elements of  $[M]$  are perturbed by Earth's oblateness  $J_2$  and atmospheric drag, as described in Ref. 3, for example.

#### Orbital Debris Collision Probability and Lifetimes

Following a breakup of an orbiting spacecraft, the short-term characteristics of the debris cloud can be determined accurately. For a low-altitude breakup, atmospheric drag begins to play a significant role in the debris cloud characteristics. In the long term, this force not only spreads out the cloud, but cleanses orbital space by removing particles as their orbits drop in altitude. Of significant concern to the space user is the collision hazard posed to a spacecraft by a debris cloud. These concerns generally can be examined as follows.

#### Probability of Collision

The probability that a spacecraft will collide with a particle in the cloud can be obtained from the relation<sup>6</sup>

$$\begin{aligned} p(\text{col}) &= 1 - \exp(-\rho v_r A t) \\ &\approx \rho v_r A t \\ &= F A t \quad \text{for } F A t \ll 1 \\ &= \rho d A \end{aligned} \quad (15)$$

Program DEBRIS computes the entry and exit times for a spacecraft passing through the cloud (Fig. 10), its relative velocity, and, therefore, distance  $d$ . The probability of colli-

sion then is obtained per unit area of the spacecraft and compared with that resulting from the micrometeoroid environment for particles of 1 mm and larger.

#### Debris LIFETIME

By inclusion of atmospheric drag, the current number of particles from a breakup in orbit and a more accurate prediction of the collision probability can be made.

A software program, LIFETIME, developed by C. C. Chao, numerically integrates the equations of motion and uses Walker and analytical representation of the Jacchia 1964 model. The Jacchia 1964 model accounts for the 11-year solar cycle, the magnetic storm effects, the 27-day effects, and the semiannual effects. The Walker analytical representation is described in Ref. 7. Also included in this dynamic model are Earth oblateness  $J_2$  effects.

#### Example

An isotropic breakup is simulated with the satellite that is breaking up in a circular orbit. Debris particles are spread at a known velocity relative to the point at which the breakup occurs. Through selection of a ballistic coefficient and atmospheric characteristics ( $F_{10.7}$ , the solar flux index and  $a_p$ , the magnetic storm index), the lifetimes of the particles can be determined. Figure 11 is a typical re-entry curve. This figure shows the lifetime characteristic of a large number of particles in a 300-km circular orbit. The solar flux index is 75, which represents a quiet atmosphere. The isotropic breakup is spreading particles with a ballistic coefficient ( $B_c = W/C_D A$ ) of 10 lb/ft<sup>2</sup> at a relative velocity of 100 m/s. After about 450

$$F_{10.7} = 75, \Delta V = 100 \text{ m/sec}$$

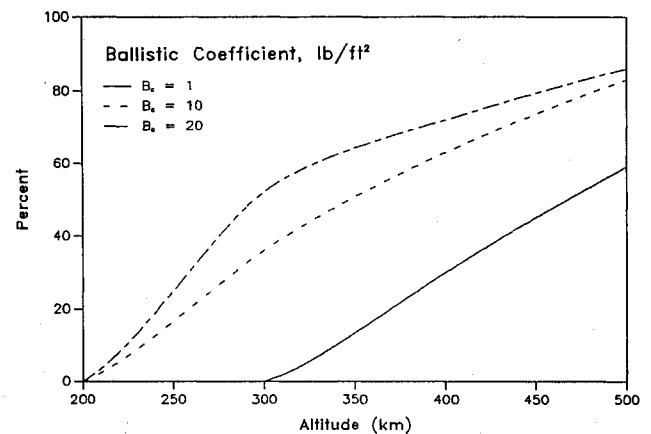


Fig. 13 Percent of particles remaining after three months.

$$F_{10.7} = 75, \Delta V = 100 \text{ m/sec}$$

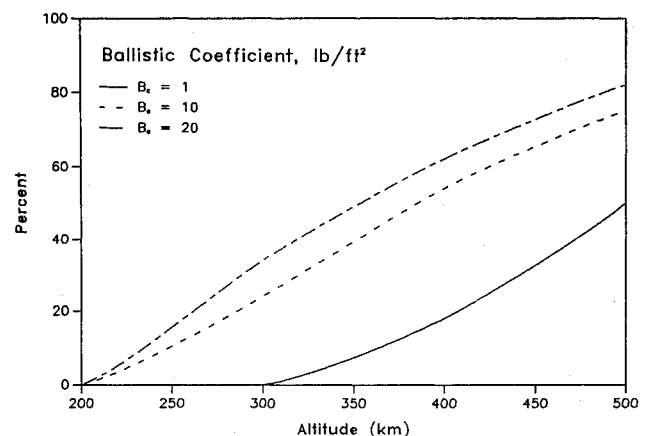


Fig. 14 Percent of particles remaining after six months.

$$F_{10.7} = 75, \Delta V = 100 \text{ m/sec}$$

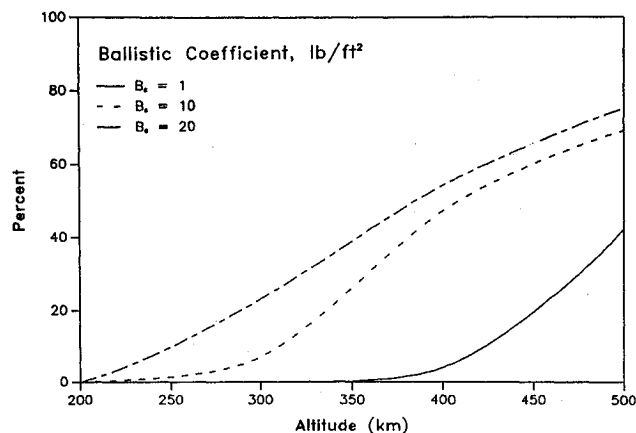


Fig. 15 Percent of particles remaining after one year.

days, 100% of these particles have re-entered. It is possible to fit a curve through the data for all the particles, thus providing a statistical representation of the decay rate.

In this study, several snapshots in time are examined. Figure 12 shows what percentage of particles of different ballistic coefficients remain, one month following a breakup, from a breakup at a given altitude, a known spread velocity, and known atmospheric characteristics. The particles with higher ballistic coefficients remain in orbit longer. These are typically the heavier, denser materials, such as structural supports. The particles with lower ballistic coefficients re-enter faster, as expected. These are typically pieces such as solar panels or insulation. The area between the extremes of ballistic coefficients represents the envelope of percent vs altitude.

Figure 13 is the same as Fig. 12, except that three months have elapsed since the breakup. In Figure 14, six months have elapsed since the breakup; in Fig. 15, one year has elapsed.

### Summary and Conclusions

An approach to modeling breakups of objects in orbit and a description of the resulting debris cloud have been presented. The results are in the form of algorithms that were implemented in programs IMPACT and DEBRIS, respectively. The output of program IMPACT includes number and velocity distributions of fragments for a direct (head-on),

partial (glancing-blow) collision or a high-intensity explosion. The debris cloud was modeled as an expanding spheroid that becomes a torus centered on the original circular target orbit. The cross-sectional area of the torus was expressed in terms of the initial spread velocities of the fragments and orbit rate. An example of the lifetime of the fragments for a satellite breaking up in a circular orbit was given for three different ballistic coefficient cases.

The IMPACT and DEBRIS programs described briefly in this paper provide a means for an approximate evaluation of the short-term collision hazard to resident space objects after an orbital breakup. A more complete description of the theory and its implementation can be found in the references cited. Further development and incorporation of future laboratory and orbital test data will provide additional improvement of the breakup and the hazard assessment models described.

### Acknowledgments

The authors wish to acknowledge the contributions of C. G. Johnson, D. L. Schmitt, and R. P. Gupta in the development of program IMPACT. The contributions of R. F. Smith, R. G. Hopkins, and D. T. Knapp in developing program DEBRIS also are acknowledged. Special thanks go to C. C. Chao, A. B. Jenkin, and A. O. Morse for reviewing the original manuscript and for their suggestions.

### References

- <sup>1</sup>Su, S. Y., and Kessler, D. J., "Contribution of Explosion and Future Collision Fragments to the Orbital Debris Environment," *Advances in Space Research*, Vol. 5, No. 2, 1984, pp. 25-34.
- <sup>2</sup>Nebolsine, P. E., Lord, G. W., and Leguer, H. H., "Debris Characterization," Teledyne Brown Engineering, PSI TR-399, Huntsville, AL, Dec. 1983.
- <sup>3</sup>Chobotov, V. A., Spencer, D. B., Schmitt, D. L., Gupta, R. P., Hopkins, R. G., and Knapp, D. T., "Dynamics of Debris Motion and the Collision Hazard to Spacecraft Resulting from an Orbital Breakup," The Aerospace Corp., TR-0086A(2430-02)-1, El Segundo, CA, Jan. 1988.
- <sup>4</sup>Chobotov, V. A., "Dynamics of Orbital Debris Clouds and the Resulting Collision Hazard to Spacecraft," *Journal of the British Interplanetary Society*, Vol. 43, No. 5, 1990, pp. 187-195.
- <sup>5</sup>Chobotov, V. A., and Wolfe, M. G., "The Dynamics of Orbiting Debris and the Impact on Expanded Operations in Space," *Journal of Astronautical Sciences*, Vol. 38, No. 1, 1990, pp. 29-39.
- <sup>6</sup>Chobotov, V. A., "Classification of Orbits with Regard to Collision Hazard in Space," *Journal of Spacecraft and Rockets*, Vol. 20, No. 5, 1983, pp. 484-490.
- <sup>7</sup>Bruce, R. W., "Atmosphere Models," The Aerospace Corp., Rept. No. TOR-1001(2307)-24, El Segundo, CA, Oct. 1966.